Assessing the Reproducibility of Labelled Antibody Binding in Quantitative Multiplexed Immuno-Mass Spectrometry-Imaging

Monique G. de Mello[a], Mika T. Westerhausen[a], Prashina Singh[a], Philip A. Doble[a], Jonathan Wanagat[b]*, David P. Bishop[a]*

[a]Atomic Medicine Initiative, Faculty of Science, University of Technology Sydney, P.O. Box 123, Broadway, NSW 2007, Australia.

[b]Division of Geriatrics, Department of Medicine, David Geffen School of Medicine at UCLA, Los Angeles, USA

*Corresponding authors - these authors contributed equally

Email: david.bishop@uts.edu.au, jwanagat@mednet.ucla.edu

Abstract

Immuno-mass spectrometry imaging (iMSI) uses laser ablation-inductively coupled plasma-mass spectrometry (LA-ICP-MS) to determine the spatial expression of biomolecules in tissue sections following immunolabelling with antibodies conjugated to a metal reporter. As with all immunolabelling techniques, the binding efficiency of multiplexed staining can be affected by a number of factors including epitope blocking and other forms of steric hindrance. To date, the effects on the binding of metal-conjugated antibodies to their epitopes in a multiplexed analysis have yet to be quantitatively explored by iMSI. Here we describe a protocol to investigate the effects of multiplexing on reproducible binding using the muscle proteins, dystrophin, sarcospan and myosin as a model, with antibodies conjugated with Maxpar® reagents before histological application to murine quadriceps sections using standard immunolabelling protocols and imaging with LA-ICP-MS. The antibodies were each individually applied to eight sections, and multiplexed to another eight sections. The average concentration of the lanthanide analytes was determined, before statistical analyses found there was no significant difference between the individual and multiplexed application of the antibodies. These analyses provide a framework for ensuring reproducibility of antibody binding during multiplexed iMSI, which will allow quantitative exploration of protein-protein interactions and provide a greater understanding of fundamental biological processes during healthy and diseased states.

Key words: LA-ICP-MS imaging, multiplexing, immuno-mass spectrometry imaging.

Acknowledgements

DPB was supported by an Australian Research Council Discovery Early Career Researcher Award DE180100194, and PAD by an Australian Research Council Discovery Project Grant DP190102361, JW is supported by National Institutes of Health Grants, R01AG055518, K02AG059847, and, and JW, PAD and DPB are supported by the National Institute of Health R21 Exploratory/Development Grant 1R21AR072950.

Introduction

Determining the role of proteins in biological processes and exploring protein-protein interactions is fundamental to understanding disease progression and mitigation. There are many chemical and biological techniques that provide information on either the quantity or the location of specific proteins, however are unable to provide the spatially resolved quantification necessary for these investigations. Furthermore, the complexity of biological samples and low levels of protein expression present another challenge [1]. Bulk tissue sampling techniques such as two-dimensional electrophoresis or nano-liquid chromatography-tandem mass spectrometry may deliver useful information regarding the concentration of proteins; however, they are unable to localise protein-protein interactions that is often crucial for elucidating function. Immunohistochemistry/ immunofluorescence (IHC/IF) provide the necessary *in situ* localisation, but are not quantitative, and are often difficult to multiplex to the degree required for investigating protein interactions.

Immuno-mass spectrometry imaging (iMSI) is an expanding field that uses immunolabelling with metal-conjugated antibodies and laser ablation-inductively coupled plasma-mass spectrometry (LA-ICP-MS) to quantitatively image biomolecules. LA-ICP-MS imaging is a solid sampling technique that involves the sequential ablation of rastered lines across a sample, with the ablated material swept into the ICP-MS with the aid of a carrier gas. The material is atomised and ionised before the detection of the elements of interest. LA-ICP-MS is an established technique for quantitatively imaging endogenous and exogenous metals; however, biomolecule detection requires the application of antibodies against target antigens to identify their location, and an elemental tag for detection. Lanthanides are typically used as tags due to 100% ionisation and high detection sensitivity, and are not typically present in biological systems resulting in low background signals and limits of detection [2]. Maxpar® reagents are commercially available enriched-isotope lanthanide tags developed for mass cytometry [3] and imaging mass cytometry (IMC)™, a form of iMSI that uses a purpose-built laser and an inductively coupled plasma-time of flight-mass spectrometer to obtain images at cellular resolution [4]. It is a straight forward procedure to conjugate the lanthanides, which are bound in a polymer, to the antibody via a reduction of the disulphide bonds of the antibody followed by a maleimide conjugation to the polymer [5]. Following conjugation, the antibody is applied to the tissue section using standard immunolabelling protocols and imaged with LA-ICP-MS. This approach was used to simultaneously image and quantify the expression of multiple proteins in myocardial infarction [6], cancerous tissue [2], and retinas [7]. The ICP-TOF used in IMC allows for highly multiplexed analyses of proteins; the first application imaged 32 targets in breast cancer biopsies [4], with recent methods analysing up to 40 targets on a single sample[8] and the inclusion of mRNA targets [9].

Bodenmiller [10] recently discussed the challenges and complexity of implementing highly multiplexed epitope-based imaging approaches, highlighting the challenges of optimising antigen retrieval and the necessity of benchmarking the antibody's performance. Benchmarking a highly multiplexed antibody panel is a laborious process. Geisen et al. [4] applied a panel of 32 antibodies to breast cancer samples and imaged via IMC. After determining that the Maxpar-conjugation to the antibodies only produced a small yet significant difference in fluorescent intensity for 6 of the antibodies, they assessed two targets via IHC, duplex IF, and IMC to see if they visually yielded similar staining patterns [4]. Ijsselsteign et al. [8] and Guo et al. [11] conducted a systematic investigation into the specificity of Maxpar-conjugated antibodies for formalin-fixed paraffin-embedded (FFPE) tissue and fresh-frozen tissue respectively, comparing each conjugated antibody individually by IHC and IMC. Ijsselstein et al. [8] assessed 65 antibodies before settling on a panel of 40, and Guo et al. [11] 80 antibodies before using a final panel of 34. Incompatible sample preparation was the main factor, however both studies observed antibodies that performed well with IHC but were not observed by IMC, and other antibodies that were not seen via IHC, which suggested the conjugation affected the antibody-binding domains. Warren et al. [12] evaluated the Maxpar-conjugated antibodies by

assessing inter- and intra-batch variability of the antibody-conjugates. A good intra-batch variation was observed; however, a large inter-batch variation may have been produced by differences in antibody yield or the degree of conjugation [12]. These studies qualitatively showed that multiplexing with conjugated primary antibodies may result in changes in specificity and sensitivity, however did not quantitatively assess whether the antibodies are reproducibly binding in a manner similar to the application of a single antibody. It is known that steric interactions may prevent antibody binding, especially when the antibody targets are in proximity [13,14], therefore, it is necessary to quantitatively interrogate the impact of highly multiplexed imaging.

Here we present a standard protocol for determining the quantitative, reproducible binding of antibodies during multiplexed iMSI. The three targets chosen as models – myosin, dystrophin and sarcospan – are proteins that occur in muscle myofibres. Dystrophin and sarcospan are members of the transmembrane dystrophin-glycoprotein complex (DGC), and are therefore present in similar locations. Myosin is a marker of the cell cytoplasm and should not interact with the other targets. The DGC is of interest due to its role in Duchenne muscular dystrophy (DMD), a terminal childhood illness that is the result of the absence or reduction in dystrophin expression, affecting all members of the complex. A growing area of interest in DMD research is understanding the relation between dystrophin and other proteins in the dystrophin-glycoprotein complex [15], as improved knowledge of the DGC function and stoichiometry in the skeletal muscle may provide an increased understanding of the contraction-induced sarcolemma injury model of DMD [16]. However, these investigations may be complicated by steric hindrance from adjacent binding sites [17] or other proteins blocking access to the antigen [18]. Antibodies for dystrophin, sarcospan, and myosin were conjugated with Maxpar® reagents and applied to eight murine quadriceps sections individually and eight sections multiplexed before imaging via LA-ICP-MS. The analysis was validated according to standard bioassay guidelines [19], and descriptive statistical analysis was conducted to determine if there were differences in the antibody concentrations on the individual and multiplexed samples.

Materials and Methods

Reagents

The anti-dystrophin (Mandys8), anti-sarcospan (E-2), and anti-myosin (MY-32) monoclonal antibodies were supplied by Santa Cruz Biotechnology (Dallas, Texas, USA). The anti-dystrophin antibody was conjugated with Maxpar® ^{158}Gd reagent by Fluidigm (South San Francisco, CA, USA). The anti-sarcospan and anti-myosin antibodies were conjugated in-house with Maxpar® ^{162}Dy and ^{146}Nd respectively according to the Fluidigm protocol. The concentration of the antibody-conjugates were determined by measuring the absorbance at 280 nm, and as per the protocol were diluted to 0.5 mg mL^{-1} for storage at 4°C. Bloxall and mouse on mouse (M.O.M.) basic kit were purchased from Vector Laboratories (Burlingame, CA, USA), Superblock and Tween-20 from Thermo Fisher Scientific (Waltham, MA, USA) and 10x TBS from Bio-Rad (Hercules, CA, USA). 0.1% TBST was prepared from TBS and Tween-20.

Seastar Baseline nitric acid, (NO_3) and 1,000 µg mL^{-1} standards of Dy, Gd, and Nd were supplied by Choice Analytical (Thornleigh, New South Wales, Australia). Tris-HCl (pH 7.4), ethylenediaminetetraacetic acid (EDTA; 10 mM), polyethylene glycol (Mn 400) and gelatine from bovine skin (100 mg; Type B) were purchased from Sigma Aldrich (Castle Hill NSW, Australia).

Grace Bio-Labs (Bend, OR) supplied 6 Hybriwell™ gasket (20x9.8 mm) and clear polycarbonate cover with two ports (item number 612107, depth 0.25 mm, volume 50 µL).

Mouse models

Wild-type mouse quadriceps tissues were harvested from mice maintained under guidelines established by the Institutional Animal Care and Use Committee at the University of California, Los Angeles, and approval for the mice in this study was granted by the UCLA Animal Welfare Assurance. Muscles were frozen in OCT, sectioned at 10 µm thickness, and stored at -80°C until immunolabelling.

Immunolabelling

The tissue samples were stained over the course of three days. On each day replicates were individually immunolabelled with the antibodies (i.e. sections with anti-dystrophin, sections with anti-sarcospan, and sections with anti-myosin), and sections were multiplexed with all three antibodies. The multiplexed mouse quadriceps sections were air-dried, washed twice with TBS, and incubated with M.O.M. blocking reagent for 60 min. Samples were then washed twice with TBST before a 5 min incubation with M.O.M. diluent, followed by sequential 30 min incubations with the conjugated primary antibodies (anti-dystrophin 1:100, anti-myosin 1:200, anti-sarcospan 1:100). The slides were then washed with TBST, rinsed with double distilled H_2O, and allowed to air dry overnight. The individually applied sections underwent the same protocol using the same antibody dilutions for direct comparison, with TBST applied in place of the antibody during the second and third incubations so that the individual protocol contained the same number of washes as the multiplexed protocol.

LA-ICP-MS

An Elemental Scientific Lasers NWR193 laser ablation system (Kennelec Scientific, Mitcham, Victoria, Australia) coupled to an Agilent Technologies 7700 Series ICP-MS (Agilent Technologies, Mulgrave, Victoria, Australia) was used for all experiments. Laser ablation and ICP-MS conditions were optimised by ablating a NIST 612 Trace Element in Glass CRM to tune for maximum sensitivity while ensuring low oxide formation (ThO/Th<0.3%, see Table 1) using our standard conditions for elemental bioimaging [20]. The ICP-MS was set to monitor isotopes ^{146}Nd, ^{158}Gd, and ^{162}Dy during ablation with a 15 µm spot size scanned at 60 µm s^{-1} with the laser set at 20 Hz and 5% power. A 300 µm x 300 µm square was ablated in each sample in approximately the same location on the consecutive tissue sections. For super resolution reconstruction (SRR) LA-ICP-MS imaging, a 15 µm spot size was scanned at 30 µm s^{-1} with the laser set at 20 Hz and 5% power. Raw data was then processed with an in-house MATLAB code and FIJI as per Westerhausen et al. [21].

Table 1. Optimised parameters for LA-ICP-MS imaging analysis.

Laser ablation	**Conditions**
Wavelength	193 nm
Laser power	5%
Laser power density (energy)	1900mJ
Laser bean diameter	15 µm
Scan speed	60 µm/s
Fequency	20 Hz
ICP-MS	
RF power source	1350 W
Carrier gas flow	1.05
Sample depth	4 mm
Extract lens 1 and 2	4.5 V, -125 V
Omega bias, lens	-80 V, 13.2 V
Octopole RF	180 V
Octopole bias	-18 V
Collision gas	H_2, 3.1 mL/min

External calibration

External calibration standards were prepared according to a previously validated protocol [22]. Briefly, a multi-elemental mix was prepared in a buffer containing 100 mM Tris-HCl buffer (pH 7.4), 10 mM EDTA, and 1% w/w polyethylene glycol in ultra-purified water (18.2 MΩ cm^{-1} at 25°C, Arium Pro Vf, Sartorius, Goettingen, Germany). Six 10% gelatine solutions were prepared in the same buffer, and spiked with differing levels of the multi-element mix. The gelatine standards were heated to 54°C until aqueous, vortexed for homogenisation, and pipetted into a 6-well hybriwell on a standard microscope slide before immediate freezing at -20°C for 15 min. The mould was then removed and the gelatine standards were stored at room temperature until analysis. An aliquot of each gelatine standard was digested in HNO_3 for characterisation via solution nebulisation ICP-MS. The calculated concentrations of the standards were 0.00, 0.14, 0.47, 1.16 and 2.32 µg mL^{-1} for Gd; 0.06, 0.25, 0.51, 1.13 and 2.10 µg mL^{-1} for Nd, and 0.64, 0.25, 0.49, 0.98 and 1.90 µg mL^{-1} for Dy.

DATA analysis and Imaging

An in-house developed MATLAB script was used to construct and calibrate the images. Data files were exported as .csv and then 3 level K-means's clustering was applied to the images for segmentation, with the concentration obtained by averaging the upper two clusters [23]. Final images were prepared in Fiji ImageJ (LOCI, University of Wisconsin, USA). Origin Pro 2019 (Originlab Corporation, Northampton, USA) [24] and cardinal packages in R for statistics (RStudio, Boston, USA) were used to process the quantitative data for statistical analysis and prepare Figures.

Figures of merit and statistical analysis

The method was validated according to the United States Food and Drug Administration guidelines, with the linearity, lower limit of quantification (LLOQ) [19], and % residual standard deviation calculated. The average values of the metal conjugate obtained from across the individual antibody sections were statistically compared against those measured on the multiplexed antibody sections by applying a two-tailed t-test at a 95% confidence interval using Originlab software. Before the t-tests were performed, the data was assessed for normality (Shapiro-Wilk at p=0.05) to confirm that it originated from a normally distributed population, a Grubb's test was applied to identify potential outliers, and an F-test to determine if the standard deviation between the two populations were similar.

Results and Discussion

Quantification of the lanthanides as a proxy of the antibodies was performed via external calibration using gelatine standards prepared and characterised according to a previously validated method [22]. The gelatine standards were run daily at the start of each analysis, with correlation coefficients greater than 0.99 obtained for all elements. The lower limit of quantification (LLOQ) was calculated using 5x signal-to-noise and ranged from 0.204-1.80 µg kg^{-1} (Table 2). The samples were analysed over eleven days and representative images of the individually applied antibodies and the multiplexed antibodies are provided in Figure 1. The average concentrations were calculated after image segmentation using K-means clustering to separate the positive signal from null values in areas of the tissue section that did not express the target biomolecules [23]. Figure 2 shows the colocalisation (white) of dystrophin (cyan) and sarcospan (magenta) in the cell membranes obtained using super resolution reconstruction to improve the image resolution from the 125 μm^2 shown in Figure 1 to 3.1 μm^2 [21], and the fast twitch fibres are identified by the myosin locations (yellow) [25]. This image is not quantified as presenting each target as a single colour necessary for colocalisation does not allow for a colour gradient that is readily interpreted.

Table 2. Analytical Figures of merit and statistical values.

Label (target)	Antibody application	Concentration (µg kg^{-1})	%RSD	G[a]	F[b]	|t|[c]	LLOQ (µg kg^{-1})	R^2
^{162}Dy (sarcospan)	Individual	41.7	24.3	0.291	0.384	0.039	0.204	0.995
	Multiplex	55.0	25.5	0.714				
^{158}Gd (dystrophin)	Individual	30.5	27.2	2.00	0.600	0.115	0.640	0.998
	Multiplex	24.3	27.7	0.264				
^{146}Nd (myosin)	Individual	42.5	15.7	0.419	0.219	0.305	1.80	1.00
	Multiplex	38.0	27.8	0.552				

[a] G < critical value G=2.215 for two-sided test (P=0.05), there is no significant outliers.

[b] F < critical value F=4.357 for two-tailed test (P=0.05), the two populations variances are not significantly different.

[c] $|t|$ < critical value t=2.306 for two-tailed test (P=0.05), the difference of the population mean is not significantly different from the test difference.

The average concentrations obtained from the individual and multiplexed applications of the antibodies are presented in Table 2. The concentrations ranged from 24.3 µg kg^{-1} (Gd) to 55.0 µg kg^{-1} (Dy). A total of 36 non-consecutive tissue sections were stained and analysed using the same antibody dilutions to facilitate direct comparison, and the %RSDs of 15.7-27.8% reflect natural biological variation. As a measure of immunolabelling robustness, the tissue sections were stained over three days, and Figure 3 represents the variation in the concentrations obtained with no clear pattern or clustering observed. To statistically compare the individual and multiplexed sample sets, the distribution of the curve was investigated and based on the normality test all were determined to follow a Gaussian or normal distribution at p=0.05. No outliers were determined for any of the analytes (Grubb's test, p=0.05), and the variances between the individual and the multiplexed sample sets were equal for the three targets (F-test, p=0.05), further demonstrating that immunolabelling samples over multiple days did not influence the analysis. A two-tailed Student's t-test was then applied to determine if the individual and the multiplexed samples were from the same population and did not show any significant difference at p=0.05, indicating that in this circumstance multiplexing did not affect quantitative binding of the three model targets.

This study was designed to establish procedures that determine if the binding of antibodies to their targets for quantitative multiplexed iMSI analysis is reproducible. The method was validated and showed sufficient sensitivity to quantify the expression of low abundant membrane proteins. A statistical comparison of the antibody concentrations after application to samples individually or in a multiplexed analysis did not show a significant difference. The multiplexed analysis contained antibodies against three targets, myosin, which should not have interferences preventing the antibody binding, and dystrophin and sarcospan, which are in close vicinity to each other and therefore with potential for steric hindrance to reduce quantitative binding of the antibodies. Steric hindrance is known to affect the binding of antibodies to protein antigens [13], therefore, it is important to determine if these interactions are occurring in a way that reduce quantitative analysis. Many antibodies are flexible and can conform their shape to bind to their target [26], however, conjugating large tags to antibodies, such as the Maxpar™ polymers that are currently used for iMSI, is known to reduce antibody binding [27]. The comparison of individually applied antibodies versus multiplexed is one amongst a number of available steric hindrance controls. Probe swapping, stain order, and "drop" control protocols allow for problem probes to be isolated to maximise the accuracy and sensitivity of the signal between individual and multiplexed staining [28-30].

Quantitative biomolecule localisation via iMSI is a field in its infancy, with fundamentals still being established [31]. There are a number of challenges to overcome before iMSI can provide bench to bedside diagnostic and prognostic information, with reproducible binding of the conjugated

antibodies crucial to the data obtained [10]. Here we have shown a standard protocol for determining if multiplexing is affecting the reproducibility of antibodies binding to their epitopes, with methods and statistics that are readily scalable as more antibodies are added to the panel for analysis.

Conclusion

The expression of three muscle proteins, dystrophin, sarcospan, and myosin, were quantified in murine skeletal muscle using iMSI after antibodies were applied individually or multiplexed. A statistical comparison of the concentrations obtained did not identify changes in concentrations between the two sample sets. The standard protocol for examining reproducible multiplexed analysis presented here is readily scalable to include a greater number of targets with well characterised antibodies, and is readily adapted across samples and target biomarkers. A highly multiplexed analysis of biomarkers has potential to speed up diagnosis and prognosis for a number of diseases where the precise location and quantitative expression of a number of protein targets is necessary such as with muscular dystrophies.

Declarations

The authors have no conflicts of interest to declare.

Wild-type mouse quadriceps tissues were harvested from mice maintained under guidelines established by the Institutional Animal Care and Use Committee at the University of California, Los Angeles, and approval for the mice in this study was granted by the UCLA Animal Welfare Assurance.

References

1. Konz I, Fernandez B, Fernandez ML, Pereiro R, Sanz-Medel A (2012) Laser ablation ICP-MS for quantitative biomedical applications. Anal Bioanal Chem 403 (8):2113-2125. doi:10.1007/s00216-012-6023-6
2. Giesen C, Mairinger T, Khoury L, Waentig L, Jakubowski N, Panne U (2011) Multiplexed immunohistochemical detection of tumor markers in breast cancer tissue using laser ablation inductively coupled plasma mass spectrometry. Anal Chem 83 (21):8177-8183. doi:10.1021/ac2016823
3. Bandura DR, Baranov VI, Ornatsky OI, Antonov A, Kinach R, Lou X, Pavlov S, Vorobiev S, Dick JE, Tanner SD (2009) Mass cytometry: technique for real time single cell multitarget immunoassay based on inductively coupled plasma time-of-flight mass spectrometry. Anal Chem 81 (16):6813-6822. doi:10.1021/ac901049w
4. Giesen C, Wang HA, Schapiro D, Zivanovic N, Jacobs A, Hattendorf B, Schuffler PJ, Grolimund D, Buhmann JM, Brandt S, Varga Z, Wild PJ, Gunther D, Bodenmiller B (2014) Highly multiplexed imaging of tumor tissues with subcellular resolution by mass cytometry. Nat Methods 11 (4):417-422. doi:10.1038/nmeth.2869
5. Lou X, Zhang G, Herrera I, Kinach R, Ornatsky O, Baranov V, Nitz M, Winnik MA (2007) Polymer-based elemental tags for sensitive bioassays. Angew Chem Int Ed Engl 46 (32):6111-6114. doi:10.1002/anie.200700796
6. Aljakna A, Lauer E, Lenglet S, Grabherr S, Fracasso T, Augsburger M, Sabatasso S, Thomas A (2018) Multiplex quantitative imaging of human myocardial infarction by mass spectrometry-immunohistochemistry. Int J Legal Med 132 (6):1675-1684. doi:10.1007/s00414-018-1813-9
7. Lores-Padin A, Fernandez B, Alvarez L, Gonzalez-Iglesias H, Lengyel I, Pereiro R (2021) Multiplex bioimaging of proteins-related to neurodegenerative diseases in eye sections by laser ablation - Inductively coupled plasma - Mass spectrometry using metal nanoclusters as labels. Talanta 221:121489. doi:10.1016/j.talanta.2020.121489

8. Ijsselsteijn ME, van der Breggen R, Farina Sarasqueta A, Koning F, de Miranda N (2019) A 40-Marker Panel for High Dimensional Characterization of Cancer Immune Microenvironments by Imaging Mass Cytometry. Front Immunol 10:2534. doi:10.3389/fimmu.2019.02534
9. Schulz D, Zanotelli VRT, Fischer JR, Schapiro D, Engler S, Lun XK, Jackson HW, Bodenmiller B (2018) Simultaneous Multiplexed Imaging of mRNA and Proteins with Subcellular Resolution in Breast Cancer Tissue Samples by Mass Cytometry. Cell Syst 6 (1):25-36 e25. doi:10.1016/j.cels.2017.12.001
10. Bodenmiller B (2016) Multiplexed Epitope-Based Tissue Imaging for Discovery and Healthcare Applications. Cell Syst 2 (4):225-238. doi:10.1016/j.cels.2016.03.008
11. Guo N, van Unen V, Ijsselsteijn ME, Ouboter LF, van der Meulen AE, Chuva de Sousa Lopes SM, de Miranda N, Koning F, Li N (2020) A 34-Marker Panel for Imaging Mass Cytometric Analysis of Human Snap-Frozen Tissue. Front Immunol 11:1466. doi:10.3389/fimmu.2020.01466
12. Warren C, McDonald D, Capaldi R, Deehan D, Taylor RW, Filby A, Turnbull DM, Lawless C, Vincent AE (2020) Decoding mitochondrial heterogeneity in single muscle fibres by imaging mass cytometry. Sci Rep 10 (1):15336. doi:10.1038/s41598-020-70885-3
13. Hlavacek WS, Posner RG, Perelson AS (1999) Steric effects on multivalent ligand-receptor binding: exclusion of ligand sites by bound cell surface receptors. Biophys J 76 (6):3031-3043. doi:10.1016/S0006-3495(99)77456-4
14. De Michele C, De Los Rios P, Foffi G, Piazza F (2016) Simulation and Theory of Antibody Binding to Crowded Antigen-Covered Surfaces. PLoS Comput Biol 12 (3):e1004752. doi:10.1371/journal.pcbi.1004752
15. Barresi R (2011) From proteins to genes: immunoanalysis in the diagnosis of muscular dystrophies. Skelet Muscle 1 (1):24. doi:10.1186/2044-5040-1-24
16. Marshall JL, Crosbie-Watson RH (2013) Sarcospan: a small protein with large potential for Duchenne muscular dystrophy. Skelet Muscle 3 (1):1. doi:10.1186/2044-5040-3-1
17. Stevenson S, Rothery S, Cullen MJ, Severs NJ (1998) Spatial relationship of the C-terminal domains of dystrophin and β-dystroglycan in cardiac muscle support a direct molecular interaction at the plasma membrane interface. Circ Res 82 (1):82-93. doi:10.1161/01.res.82.1.82
18. Choi ES, Rettig WJ, Wayner EA, Srour ML, Clegg DO (1994) Functional identification of integrin laminin receptors that mediate process outgrowth by human SY5Y neuroblastoma cells. J Neurosci Res 37 (4):475-488. doi:10.1002/jnr.490370407
19. Food US, Drug A (2015) Compliance program 7348.811. Chapter 48-bioresearch monitoring: researchers and sponsor-investigators. US Food and Drug Administration. doi:https://www.fda.gov/media/75909/download
20. Lear J, Hare DJ, Fryer F, Adlard PA, Finkelstein DI, Doble PA (2012) High-resolution elemental bioimaging of Ca, Mn, Fe, Co, Cu, and Zn employing LA-ICP-MS and hydrogen reaction gas. Anal Chem 84 (15):6707-6714. doi:10.1021/ac301156f
21. Westerhausen MT, Bishop DP, Dowd A, Wanagat J, Cole N, Doble PA (2019) Super-Resolution Reconstruction for Two- and Three-Dimensional LA-ICP-MS Bioimaging. Anal Chem 91 (23):14879-14886. doi:10.1021/acs.analchem.9b02380
22. Westerhausen MT, Lockwood TE, Gonzalez de Vega R, Rohnelt A, Bishop DP, Cole N, Doble PA, Clases D (2019) Low background mould-prepared gelatine standards for reproducible quantification in elemental bio-imaging. Analyst 144 (23):6881-6888. doi:10.1039/c9an01580a
23. Bishop DP, Westerhausen MT, Barthelemy F, Lockwood T, Cole N, Gibbs EM, Crosbie RH, Nelson SF, Miceli MC, Doble PA, Wanagat J (2021) Quantitative immuno-mass spectrometry imaging of skeletal muscle dystrophin. Sci Rep 11 (1):1128. doi:10.1038/s41598-020-80495-8
24. Schindelin J, Arganda-Carreras I, Frise E, Kaynig V, Longair M, Pietzsch T, Preibisch S, Rueden C, Saalfeld S, Schmid B, Tinevez JY, White DJ, Hartenstein V, Eliceiri K, Tomancak P, Cardona A (2012) Fiji: an open-source platform for biological-image analysis. Nat Methods 9 (7):676-682. doi:10.1038/nmeth.2019

25. Shang GK, Han L, Wang ZH, Liu YP, Yan SB, Sai WW, Wang D, Li YH, Zhang W, Zhong M (2020) Sarcopenia is attenuated by TRB3 knockout in aging mice via the alleviation of atrophy and fibrosis of skeletal muscles. J Cachexia Sarcopenia Muscle 11 (4):1104-1120. doi:10.1002/jcsm.12560
26. Davies DR, Cohen GH (1996) Interactions of protein antigens with antibodies. Proc Natl Acad Sci U S A 93 (1):7-12. doi:10.1073/pnas.93.1.7
27. Kent SP, Ryan KH, Siegel AL (1978) Steric hindrance as a factor in the reaction of labeled antibody with cell surface antigenic determinants. J Histochem Cytochem 26 (8):618-621. doi:10.1177/26.8.357645
28. Syed J, Ashton J, Joseph J, Jones GN, Slater C, Sharpe A, Ashton G, Howat W, Byers R, Angell HK (2019) Multiplex immunohistochemistry: the importance of staining order when producing a validated protocol. Immunotherapy 5:1000157. doi:10.35248/2471-9552.19.5.157
29. Taube JM, Akturk G, Angelo M, Engle EL, Gnjatic S, Greenbaum S, Greenwald NF, Hedvat CV, Hollmann TJ, Juco J, Parra ER, Rebelatto MC, Rimm DL, Rodriguez-Canales J, Schalper KA, Stack EC, Ferreira CS, Korski K, Lako A, Rodig SJ, Schenck E, Steele KE, Surace MJ, Tetzlaff MT, von Loga K, Wistuba, II, Bifulco CB, Society for Immunotherapy of Cancer Pathology Task F (2020) The Society for Immunotherapy of Cancer statement on best practices for multiplex immunohistochemistry (IHC) and immunofluorescence (IF) staining and validation. J Immunother Cancer 8 (1). doi:10.1136/jitc-2019-000155
30. Surace M, DaCosta K, Huntley A, Zhao W, Bagnall C, Brown C, Wang C, Roman K, Cann J, Lewis A, Steele K, Rebelatto M, Parra ER, Hoyt CC, Rodriguez-Canales J (2019) Automated Multiplex Immunofluorescence Panel for Immuno-oncology Studies on Formalin-fixed Carcinoma Tissue Specimens. J Vis Exp (143). doi:10.3791/58390
31. Bishop DP, Cole N, Zhang T, Doble PA, Hare DJ (2018) A guide to integrating immunohistochemistry and chemical imaging. Chem Soc Rev 47 (11):3770-3787. doi:10.1039/c7cs00610a

Table 1. Optimised parameters for LA-ICP-MS imaging analysis.

Laser ablation	**Conditions**
Wavelength	193 nm
Laser power	5%
Laser power density (energy)	1900mJ
Laser bean diameter	15 µm
Scan speed	60 µm/s
Fequency	20 Hz
ICP-MS	
RF power source	1350 W
Carrier gas flow	1.05
Sample depth	4 mm
Extract lens 1 and 2	4.5 V, -125 V
Omega bias, lens	-80 V, 13.2 V
Octopole RF	180 V
Octopole bias	-18 V
Collision gas	H_2, 3.1 mL/min

Table 2. Analytical Figures of merit and statistical values.

Label (target)	**Antibody application**	**Concentration (µg kg^{-1})**	**%RSD**	**G[a]**	**F[b]**	**|t|[c]**	**LLOQ (µg kg^{-1})**	**R^2**
^{162}Dy (sarcospan)	Individual	41.7	24.3	0.291	0.384	0.039	0.204	0.995
	Multiplex	55.0	25.5	0.714				
^{158}Gd (dystrophin)	Individual	30.5	27.2	2.00	0.600	0.115	0.640	0.998
	Multiplex	24.3	27.7	0.264				
^{146}Nd (myosin)	Individual	42.5	15.7	0.419	0.219	0.305	1.80	1.00
	Multiplex	38.0	27.8	0.552				

[a] G < critical value G=2.215 for two-sided test (P=0.05), there is no significant outliers.

[b] F < critical value F=4.357 for two-tailed test (P=0.05), the two populations variances are not significantly different.

[c] $|t|$ < critical value t=2.306 for two-tailed test (P=0.05), the difference of the population mean is not significantly different from the test difference.

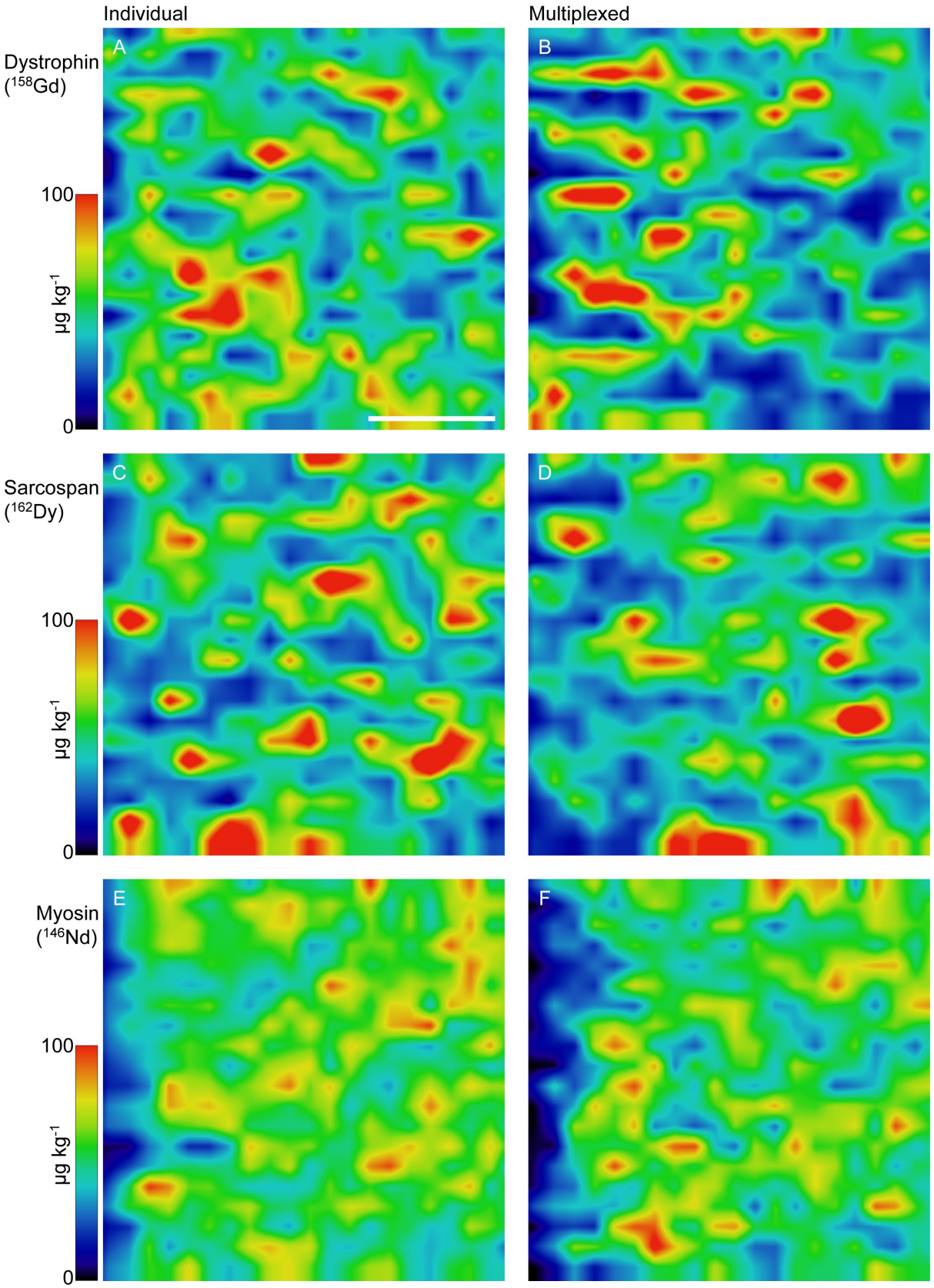

Figure 1. Representative images of individually (A, C, E) and multiplex (B, D, F) stained murine quadriceps. ^{158}Gd images representing dystrophin are shown in (A) and (B), ^{162}Dy as sarcospan in (C) and (D), and ^{146}Nd as myosin in (E) and (F). Scale bar is 100 µm.

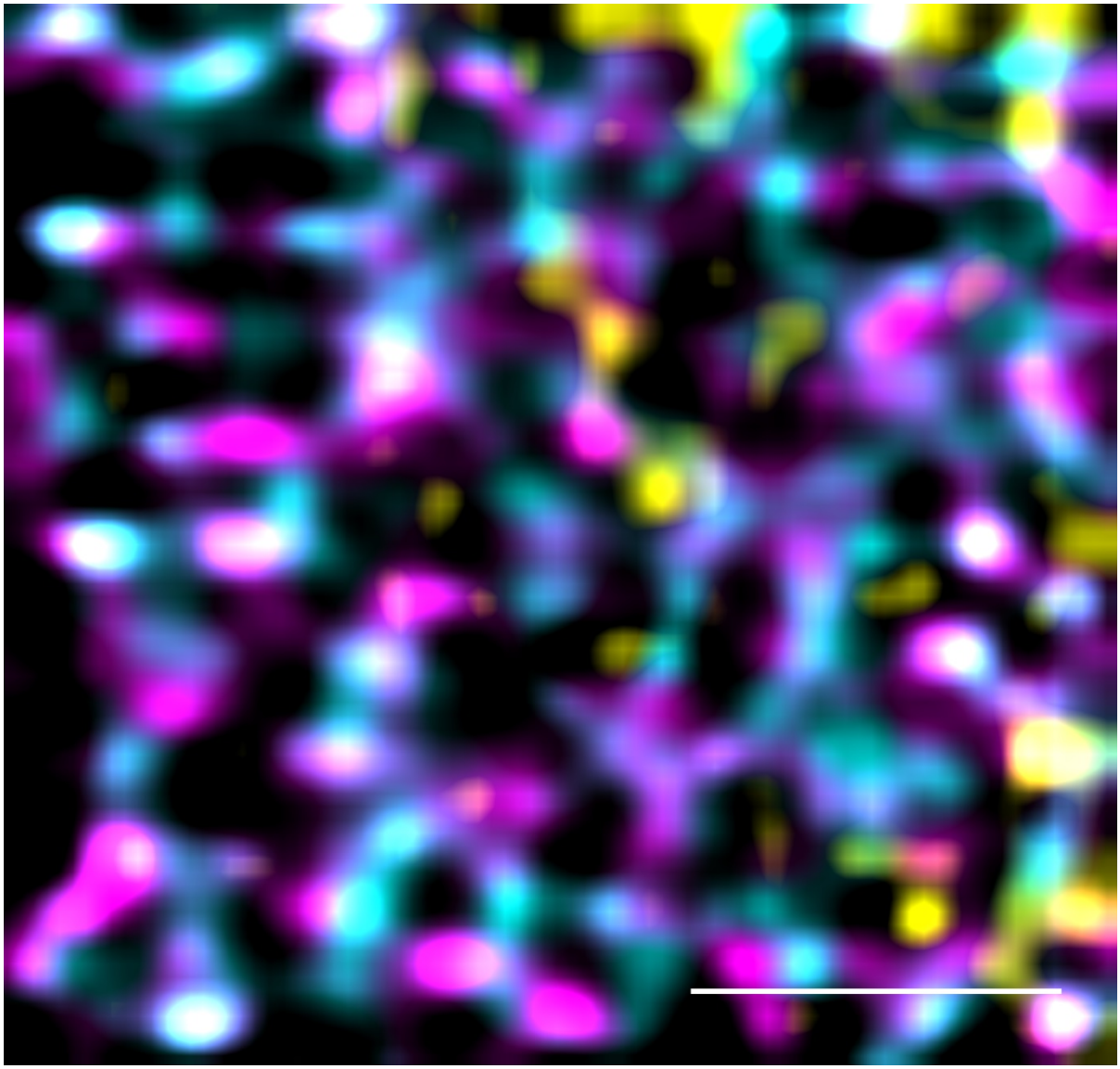

Figure 2. False colour SRR image of anti-dystrophin ^{158}Gd (cyan), anti-myosin ^{146}Nd (yellow) and anti-sarcospan ^{162}Dy (magenta) in murine quadriceps. White signifies overlapping dystrophin and sarcospan signal. Scale bar is 100 µm.

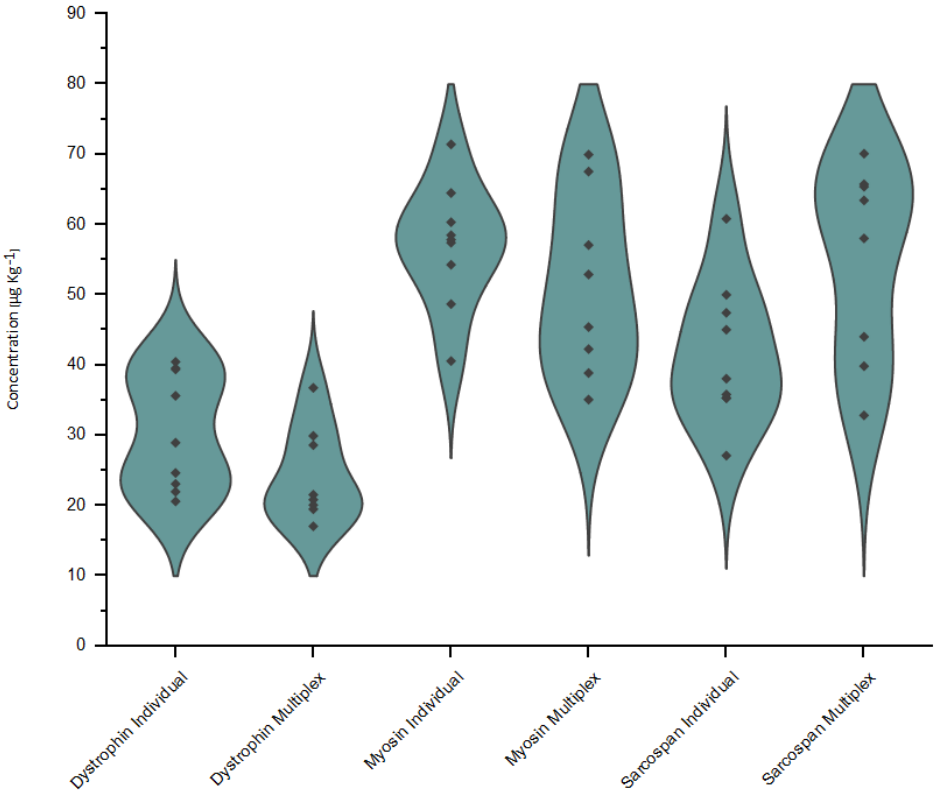

Figure 3. The average concentrations obtained of the metal proxies for each protein measured with iMSI. No statistical differences in concentration were observed between the two samples (P=0.05).